BASE SHEAR ESTIMATED FROM FLOOR ACCELERATIONS AND COLUMN SHEARS

By RAKESH K. GOEL

TABLE OF CONTENTS

TABLE OF CONTENTS	II
ABSTRACT	III
ACKNOWLEDGMENT	IV
INTRODUCTION	1
SELECTED BUILDINGS AND STRONG-MOTION DATA	6
Selected Buildings	6
20-Story Hotel in North Hollywood	
19-Story Office Building in Los Angeles	
Selected Ground Motions	
ANALYTICAL MODELS	
North Hollywood Hotel	10
Los Angeles Office Building	11
COMPARISON OF INERTIAL AND STRUCTURAL BASE SHEARS	13
Single-Degree-of-Freedom Systems	13
Multistory Buildings	15
CONCLUSIONS	20
REFERENCES	22

ABSTRACT

This paper compares base shear computed from floor accelerations (inertial base shear) and column shears (structural base shear) for several single-degree-of-freedom (SDF) systems and two mid-rise, multi-story buildings due to a suite of 30 earthquake ground motions. The presented results show that the inertial base shear is close to structural base shear in short-period (<1 sec) SDF systems but may significantly exceed the structural base shear for individual ground motions in longer period (> 1 sec) SDF systems. Furthermore, the inertial base shear exceeds the structural base shear in the median by 10% to 20% and may exceed the structural base shear by as much as 70% for individual ground motions in multi-story buildings. Therefore, it is concluded that the inertial base shear should be used with caution to estimate the structural base shear in buildings with long fundamental vibration period whose motions are recorded during individual earthquake ground shaking.

ACKNOWLEDGMENT

This investigation is supported by the California Department of Conservation, California Geological Survey, Strong Motion Instrumentation Program, Contract No. 1007-907. This support is gratefully acknowledged. The author would also like to acknowledge the support provided by Prof. Graham Powell on implementation of *Perform3D* and by Dr. Charles Chadwell and Karen Nishimoto on use of *Xtract*.

INTRODUCTION

Buildings are typically instrumented with accelerometers at selected number of floors: low-rise buildings (1 to 3 stories) at every floor; and mid- and high-rise buildings at base, roof, and a few intermediate floors. The raw (or uncorrected) acceleration recorded during earthquakes from these accelerometers are processed using well-established procedures to obtain base-line corrected accelerations (Shakal et al., 2003). The processed floor accelerations at instrumented floors are interpolated (Naeim, 1997; Naeim, et al., 2004; De la Llera and Chopra, 1998; Goel, 2005, 2007, 2009; Limongelli, 2003, 2005) to estimate accelerations at all floors. These floor accelerations are then used to estimate base shear by adding all floor inertial forces above the base (Figure 1a) with the floor inertial forces are computed as the product of floor acceleration and floor mass (e.g., Jennings, 1997; Naeim, 1997). The base shear computed using the aforementioned procedure is referred to as the "inertial base shear" in rest of this paper and is denoted by V_{bul} in the longitudinal direction and V_{byl} in the transverse direction.

The inertial base shear demand is often compared with the base shear capacity, estimated from pushover curve which is the relationship between base shear and roof displacement developed from nonlinear static pushover analysis (e.g., Goel, 2005), or the code design level base shear (e.g., Naeim, 2004). The base shear in pushover analysis is computed as the sum of shear forces in all columns at the building's base (Figure 1b). Similarly, the code design level base shear is indicative of sum of shear forces in all columns at the building's base when the code based height-wise distribution of forces are applied to the building. The base shear defined by the aforementioned procedure is referred to as the "structural base shear" in rest of this paper and is denoted by V_{bxR} in the longitudinal direction and V_{byR} in the transverse direction.

A large number of buildings are instrumented in seismically active region like California. The strong motion records obtained from such buildings during earthquake ground shaking are increasingly being used for making decision about the need for detailed post-earthquake inspection of such buildings. One of the criteria triggering detailed inspection involves comparing inertial base shear induced in the building during an earthquake ground shaking with its structural base shear capacity (or code design level shear force): if the inertial base shear

exceeds the base shear capacity, the building is expected to suffer damage and requires detailed inspection.

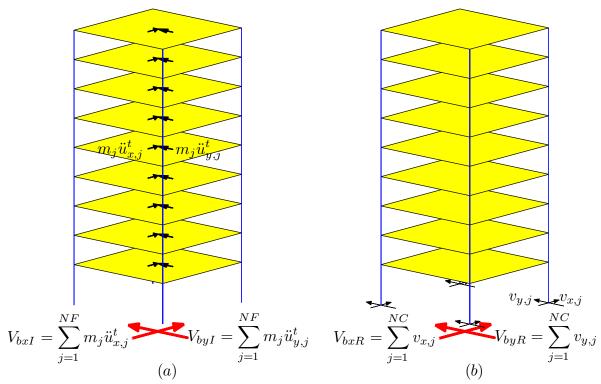


Figure 1. Computation of base shear: (a) Inertial base shear computed from summation of inertial floor forces; and (b) Structural base shear computed from summation of column shears.

Since the level of nonlinear action (or damage) is related to forces (or deformations) induced in structural members, such as structural base shear (or story drifts), the practice of comparing inertial base shear with base shear capacity or code design level base shear tacitly assumes that the inertial and structural base shears are sufficiently close. However, observations from buildings that were strongly shaken during the 1994 Northridge earthquake indicate that inertial base shear may not be a good indicator of damage in the building because it does not correlate well with the structural base shear.

In order to illustrate the lack of correlation between inertial base shear and damage (or structural base shear), consider the performance of two buildings – 20-Story Reinforced-Concrete Hotel in North Hollywood and 19-Story Steel Office Building in Los Angeles – during the 1994 Northridge earthquake. The peak recorded accelerations during the 1994 Northridge

earthquake at roof were 0.65g for both buildings. The North Hollywood Hotel was reported to have suffered insignificant damage, and the Los Angeles Building was reported to have suffered moderate damage in the form of buckling in some braces at upper floor levels (Naeim, 1997, 1998). Post-earthquake inspection report clearly indicates that these buildings were deformed either slightly beyond the linear elastic range, as may be the case for the North Hollywood Hotel, or moderately beyond the linear elastic limit, as may be the case for the Los Angeles Building. As a result, the inertial base shear demand should not have significantly exceeded the structural base shear capacity during the 1994 Northridge earthquake if the assumption of inertial base shear being close to the structural base shear were to be applicable.

Figure 2 and 3 present pushover curves for the North Hollywood Hotel and the Los Angeles Building, respectively, in the transverse and longitudinal direction. These pushover curves were generated using three-dimensional nonlinear models and height-wise distribution of forces proportional to the first mode in selected direction. Details of these buildings, nonlinear model, and analytical approach are presented later in the paper. Also included are the peak values of the inertial base shear demands for these buildings during the 1994 Northridge earthquake. The peak inertial base shear demands are available from previous publications (Naeim, 1997, 1998).

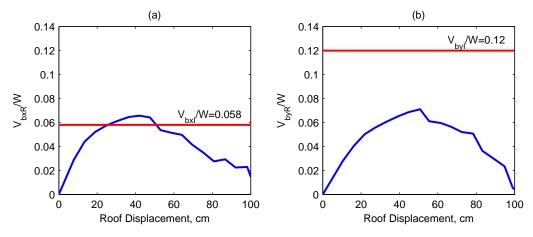


Figure 2. Comparison of structural base shear capacity obtained from pushover analysis and inertial base shear demand during 1994 Northridge earthquake for the North Hollywood Hotel: (a) Longitudinal direction, and (b) Transverse direction.

These results indicate that the peak inertial base shear reported during the 1994 Northridge earthquake significantly exceeded the peak structural base shear capacity estimated from

pushover analysis for the North Hollywood Hotel in the transverse direction (Figure 2b) and for the Los Angeles Building in both directions (Figures 3a and 3b). As noted previously, these buildings were not reported to suffer significant damage during the 1994 Northridge earthquake. Similar observations made another recent investigation (Goel and Chadwell, 2007). Therefore, there is a need for careful re-examination of correlation between inertial and structural base shears.

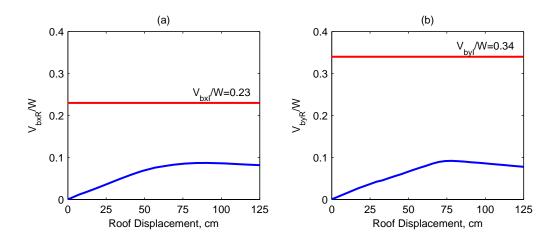


Figure 3. Comparison of structural base shear capacity obtained from pushover analysis and inertial base shear demand during 1994 Northridge earthquake for the Los Angeles Building: (a) Longitudinal direction, and (b) Transverse direction.

The discrepancy observed in Figures 2 and 3 between peak inertial and structural base shear occurs due to combination of the following three factors. First, the error may occur in estimation of peak inertial base shear because interpolation procedure used to estimate accelerations at non-instrumented floors may lead to inaccurate floor accelerations which in turn will lead to inaccurate floor inertial forces and inertial base shear. Second, the error may occur in estimation of peak structural base shear capacity because the peak structural base shear estimated from pushover analysis differs from that in the "actual" building due to errors associated with modeling and analytical assumptions. Third, inertial and structural base shears differ by contribution due to damping forces. This becomes apparent from the following dynamic equilibrium equation for a multi-degree-of-freedom building subjected to ground shaking

$$\mathbf{m}\ddot{\mathbf{u}}^t + \mathbf{c}\dot{\mathbf{u}} + \mathbf{f}_s \left(\mathbf{u}, \text{ sign } \dot{\mathbf{u}} \right) = \mathbf{0}$$
 (1)

in which $\mathbf{m}\ddot{\mathbf{u}}'$ are the inertial floor forces which lead to the inertial base shear, $\mathbf{f}_s(\mathbf{u}, \operatorname{sign} \dot{\mathbf{u}})$ are the forces in structural members which lead to the structural base shear, and $\mathbf{c}\dot{\mathbf{u}}$ are the damping forces. In Equation (1), \mathbf{m} is the mass matrix; \mathbf{c} is the damping matrix; $\ddot{\mathbf{u}}' = \ddot{\mathbf{u}} + \mathbf{r}\ddot{u}_g$ is the total acceleration vector with $\ddot{\mathbf{u}}$ being the relative acceleration vector, \mathbf{r} being the influence vector, and \ddot{u}_g being the ground acceleration; $\dot{\mathbf{u}}$ is the relative velocity vector; and \mathbf{u} is the relative displacement vector.

A comprehensive study to fully understand the contribution of each of the three factors requires that errors corresponding to each factor be examined individually. This is possible only if the building is instrumented to measure accelerations at each floor and shears in all columns at its base. Clearly, such a study requires detailed laboratory experiments on well instrumented full-scale or scaled models of multi-story buildings. Since experimental study is beyond scope of this investigation, results from numerical simulation studies are used to develop an improved understanding of difference between inertial and structural base shear in multi-story buildings. For this purpose, responses (floor accelerations, column shears) of three-dimensional computer models two building – 20-Story Reinforced-Concrete Hotel in North Hollywood and 19-Story Steel Office Building in Los Angeles – are computed from nonlinear response history analysis (RHA) for a suite of 30 ground motions recorded during past earthquakes. The inertial and structural base shears are them computed form the nonlinear RHA results and compared to understand the discrepancy between the two for multi-story buildings.

It is useful to note that the approach used in this investigation eliminates the errors associated with interpolation of accelerations because accelerations are available at all floors. Furthermore, it also eliminates the errors associated with modeling and analytical assumptions because both inertial base shear and structural base shear are for the same model, albeit a computer model.

SELECTED BUILDINGS AND STRONG-MOTION DATA

Selected Buildings

Two buildings – 20-Story Hotel in North Hollywood and 19 Story Office Building in Los Angeles – are selected in this investigation as representative of mid- to high-rise reinforced-concrete and steel buildings in California. Following is a brief description of each of these building.

20-Story Hotel in North Hollywood

This building has 20 stories above and one floor below the ground (Figure 4). Designed in 1966, its vertical load carrying system consists of 11.4 cm (4.5 inch) to 15 cm (6 inch) thick RC slabs supported by concrete beams and columns. The lateral load system consists of ductile moment resisting concrete frames in both directions. The foundation system consists of spread footing below columns. The fundamental vibration period of this building is estimated to be 2.98 sec in the transverse direction and 2.57 sec in the longitudinal direction.

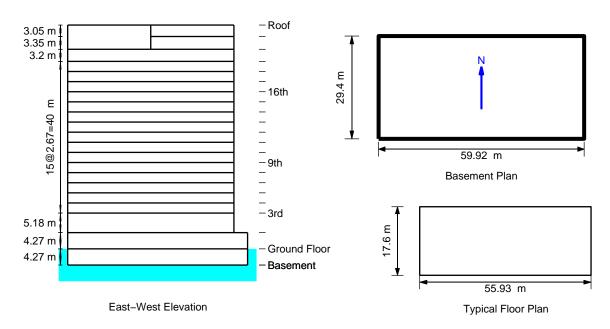


Figure 4. Elevation and plan of 20-Story Hotel in North Hollywood.

19-Story Office Building in Los Angeles

This building has 19 stories above the ground level and 4 stories of parking below the ground level (Figure 5). The building was designed in 1966-67 and constructed in 1967. The vertical load carrying system consists of 11.4 cm (4.5 in.) thick reinforced concrete slabs supported on

steel frames. The lateral load resisting system consists of four moment resisting steel frames in the longitudinal direction, and five X-braced steel frames in the transverse direction. The foundation system consists of 22 m (72 ft- 4 in) long driven-steel I-beam piles (Hart, 1973; Naeim, 1998). The piles are capped in groups of three to ten with pile caps varying in thickness from 1.12m (3 ft-8 in) to 1.73 m (5 ft – 8 in). All pile caps are connected with 0.61m by 0.61 m (2 ft by 2 ft) reinforced concrete tie beams. The subsurface soil conditions are generally fine sand throughout the depth of the piles. The fundamental vibration period of this building is estimated to be 3.52 sec in the transverse direction and 3.89 sec in the longitudinal direction.

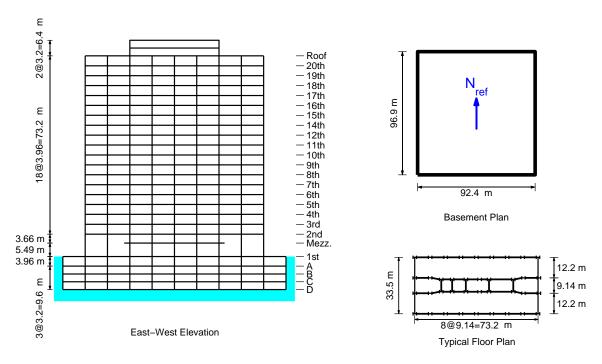


Figure 5. Elevation and plan of 19-Story Office Building in Los Angeles.

Selected Ground Motions

A suite of 30 ground motions have been selected in this investigation (Table 1). Each ground motion consists of a pair of two horizontal components of ground motion recorded during indicated earthquake. These earthquakes are selected for a wide range of parameters: proximity to the fault, magnitude, peak ground accelerations and velocities. These ground motions were not selected to match any design spectrum but to ensure that they will induce different levels of inelastic behavior in the selected buildings: selected buildings are expected to remain within the

linear elastic range for a few earthquakes where as these buildings are expected to be deformed well into the nonlinear range, and possibly collapse, during other earthquakes. Because some of the ground motions were very long and would require excessive computational time for analysis of selected buildings, truncated histories were selected for several ground motions.

Table 1. Selected ground motions.

Serial No.	Station Name	Earthquake	Mag.	Epic. Dist. (km)	PGA (H1, H2, V) -
1	Parkfield-Fault Zone 1	Parkfield, September 28, 2004	6.0	9	0.59, 0.82, 0.26
2	Parkfield-Fault Zone 14	Parkfield, September 28, 2004	6.0	12	1.31, 0.54, 0.56
3	Templeton-1-story Hospital GF	San Simeon, December 22, 2003	6.5	38	0.42, 0.46, 0.26
4	Amboy	Hector Mine, October 16, 1999	7.1	48	0.15, 0.18, 0.13
5	Taiwan-CHY028	Chi-Chi, September 21, 1999	7.6	7 to fault	0.82, 0.65, 0.34
6	Taiwan-TCU129	Chi-Chi, September 21, 1999	7.6	1 to fault	0.63, 1.01, 0.34
7	Taiwan-TCU068	Chi-Chi, September 21, 1999	7.6	1 to fault	0.46, 0.56, 0.49
8	Taiwan-CHY028	Chi-Chi, September 21, 1999	7.6	10 to fault	0.42, 1.16, 0.34
9	Sylmar-County Hospital Lot	Northridge, January 17, 1994	6.7	16	0.59, 0.83, 0.53
10	Newhall-LA County Fire Station	Northridge, January 17, 1994	6.7	20	0.57, 0.58, 0.54
11	Los Angeles-Rinaldi Rec. Station FF	Northridge, January 17, 1994	6.7	9	0.47, 0.83, 0.83
12	Santa Monica-City Hall Grounds	Northridge, January 17, 1994	6.7	23	0.88, 0.37, 0.23
13	Lucerne Valley	Landers, June 28, 1992	7.4	1 to fault	0.72, 0.78, 0.82
14	Yermo-Fire Station	Landers, June 28, 1992	7.4	84	0.15, 0.24, 0.13
15	Big Bear Lake-Civic Center Grounds	Big Bear, June 28, 1992	6.5	11	0.48, 0.55, 0.19
16	Petrolia-Fire Station	Cape Mendocino, April 26, 1992	6.6	35	0.59, 0.43, 0.15
17	Petrolia-Fire Station	Petrolia, April 25, 1992	7.1	8	0.65, 0.58, 0.16
18	Cape Medocino	Petrolia, April 25, 1992	7.1	11	1.04, 1.50, 0.75
19	Rio Dell-Hwy101/Painter Street Overpass FF	Petrolia, April 25, 1992	7.1	18	0.39, 0.55, 0.20
20	Corralitos-Eureka Canyon Road	Loma Prieta, October 17, 1989	7.0	7	0.48, 0.63, 0.44
21	Los Gatos-Linahan Dam Left Abut.	Loma Prieta, October 17, 1989	7.0	19	0.40, 0.44, 0.13
22	Saratoga-Aloha Ave.	Loma Prieta, October 17, 1989	7.0	4	0.32, 0.49, 0.35
23	El Centro-Imperial County Center Grounds	Superstition Hills, November 24, 1987	6.6	36	0.26, 0.34, 0.12
24	Los Angeles-Obregon Park	Whittier, October 1, 1987	6.1	10	0.43, 0.41, 0.13
25	Chalfant-Zack Ranch	Chafant Valley, July 21, 1986	6.4	14	0.40, 0.44, 0.30
26	El Centro-Array #6	Imperial Valley, October 15, 1979	6.6	1 to fault	0.43, 0.37, 0.17
27	El Centro-Array #7	Imperial Valley, October 15, 1979	6.6	1 to fault	0.45, 0.33, 0.50
28	El Centro-Imperial County Center Grounds	Imperial Valley, October 15, 1979	6.6	28	0.24, 0.21, 0.24
29	El Centro-Hwy8/Meloland Overpass FF	Imperial Valley, October 15, 1979	6.6	19	0.31, 0.29, 0.23
30	El Centro-Irrigation District	El Centro, May 18, 1940	6.9	17	0.34, 0.21, 0.21

ANALYTICAL MODELS

The three-dimensional analytical models of the selected buildings were developed using the structural analysis software *Perform3D* (CSI, 2006). Following is a description of modeling procedure for each of the two selected buildings.

North Hollywood Hotel

The beams were modeled with FEMA Concrete Beam with strength loss and unsymmetrical section strength, columns were modeled with FEMA Concrete Column with strength loss and symmetrical section strength, and shear walls were modeled with linear elastic column elements. The FEMA Beam element requires moment-plastic-rotation relationship of Figure 6a. The yield moment of the beam section needed to define the FEMA force-deformation behavior is computed from section moment-curvature analysis using computer program *XTRACT* (TRC, 2008).

The plastic rotation values and the residual strength needed for the FEMA Concrete Beam model in *Perform3D* are selected as per FEMA-356 (ASCE, 2000) recommendations: plastic rotations are selected as 0.02 for point U and 0.03 for point X, and the residual strength for points R and X are selected as 20% of the yield moment (Figure 6a). The plastic rotation value for point R is selected as 0.022 to model gradual strength loss between points U and R.

The FEMA Concrete Column with strength loss element requires moment-plastic-rotation behavior of Figure (2a), P-M interaction diagram for bending about axis-2 and axis-3 (Figure 6b), and M-M interaction diagram between moments about axis-2 and axis-3 (Figure 6c). The yield moment needed to define the force-deformation behavior (Figure 6a) was obtained from *XTRACT* moment-curvature analyses of column sections about axis-2 and axis-3. Similarly, the parameters needed to define P-M interaction diagrams about axis-2 and axis-3 (Figure 6b) were estimated from *XTRACT* P-M interaction analyses of columns sections. The shapes of the P-M interaction diagrams (Figure 6b) and M-M interaction diagram (Figure 6c) were defined using default values of various exponents in *Perform3D*.

Similar to the beams, the plastic rotation values and the residual strength needed for the FEMA Concrete Column model in *Perform3D* are selected as per FEMA-356 recommendations:

plastic rotations are selected as 0.02 for point U and 0.03 for point X, and the residual strength for points R and X are selected as 20% of the yield moment (Figure 6a). The plastic rotation value for point R is selected as 0.022 to model gradual strength loss between points U and R.

The damping in the model is defined as Rayleigh damping with the mass and stiffness proportional coefficient computed by specifying 6.5% damping for first mode and 15% damping for fifteenth mode. This damping model was selected to ensure that damping ratios in most significant modes match the modal damping ratios identified from system identification applied to motions of the North Hollywood Hotel recorded during the 1994 Northridge earthquake.

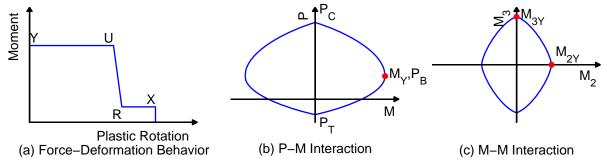


Figure 6. FEMA concrete beam/column element in *Perform3D*: (a) Force-deformation behavior of beam or column, (b) P-M interaction diagram for column; and (c) M-M interaction diagram for column.

Los Angeles Office Building

The beams were modeled with FEMA Steel Beam with strength loss and symmetrical section strength, columns were modeled with FEMA Steel Column with strength loss and symmetrical section strength, shear walls were modeled with linear elastic column elements, and braces were modeled with Simple Bar element. The material properties for braces were specified by Inelastic Steel Buckling material in Perform3D. The FEMA Steel Beam element requires moment-plastic-rotation relationship of Figure 7a. The yield moment of the steel beam section was computed automatically by Perform3D using section properties and steel strength. The plastic rotation values and the residual strength needed for the FEMA Steel Beam model in Perform3D are selected as per FEMA-356 recommendations: plastic rotations are selected as $9\theta_y$ for point U and $11\theta_y$ for point X in which θ_y is the yield rotation, and the residual strength for points R and X are selected as 60% of the yield moment (Figure 7a). The plastic rotation value for point R is

selected as $9.5\theta_{v}$ to model gradual strength loss between points U and R.

The FEMA Steel Column with strength loss element requires moment-plastic-rotation behavior of Figure (7a), P-M interaction diagram for bending about axis-2 and axis-3 (Figure 7b), and M-M interaction diagram between moments about axis-2 and axis-3 (Figure 7c). The yield moment needed to define the force-deformation behavior (Figure 7a) was automatically computed by Perform3D based on section properties and material strength. Similar to the beams, the plastic rotation values and the residual strength needed for the FEMA Steel Column model in Perform3D are selected as per FEMA-356 recommendations: plastic rotations are selected as $9\theta_y$ for point U and $11\theta_y$ for point X in which θ_y is the yield rotation, and the residual strength for points R and X are selected as 60% of the yield moment (Figure 7a). The shapes of the P-M interaction diagrams (Figure 3b) and M-M interaction diagram (Figure 7c) were also automatically generated in Perform3D based on the specified section properties and material strength.

As noted previously for the North Hollywood Hotel, the damping in the model for the Los Angeles Building is also defined as Rayleigh damping with the mass and stiffness proportional coefficient computed by specifying 2.2% damping for second mode and 5% damping for eighteenth mode. This damping model was selected to ensure that damping ratios in most significant modes match the modal damping ratios identified from system identification applied to motions of the Los Angeles Building recorded during the 1994 Northridge earthquake.

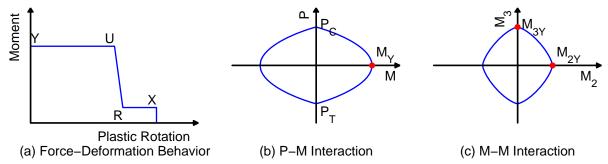


Figure 7. FEMA steel beam/column element in *Perform3D*: (a) Force-deformation behavior of beam or column, (b) P-M interaction diagram for column; and (c) M-M interaction diagram for column.

COMPARISON OF INERTIAL AND STRUCTURAL BASE SHEARS

Single-Degree-of-Freedom Systems

Prior to investigating the difference between inertial and structural base shears of multi-story building, it is useful to understand the difference for simple single-degree-of-freedom (SDF) systems responding with the linear elastic range for selected suite of ground motions. This requires solving the following equation of motion for linear elastic SDF system:

$$\ddot{u} + 2\omega_n \zeta_n \dot{u} + \omega_n^2 u = -\ddot{u}_g \tag{2}$$

in which ω_n and ζ_n are the vibration frequency (= $2\pi/T_n$ with T_n being the vibration period) and damping ratio, respectively; \ddot{u} , \dot{u} , and u, are the relative acceleration, velocity, and displacement of the system, respectively; and \ddot{u}_g is the ground acceleration. The peak inertial base shear, V_{bI} , and peak structural base shear, V_{bR} , are computed from

$$V_{bI} = \left| m \left(\ddot{u} + \ddot{u}_g \right) \right|_{\text{max}} \tag{3}$$

$$V_{bR} = \left| ku \right|_{\text{max}} \tag{4}$$

and the ratio V_{bI}/V_{bR} given by

$$\frac{V_{bI}}{V_{bR}} = \frac{\left| m \left(\ddot{u} + \ddot{u}_g \right) \right|_{\text{max}}}{\left| k u \right|_{\text{max}}} = \frac{\left| \left(\ddot{u} + \ddot{u}_g \right) \right|_{\text{max}}}{\left| \omega_n^2 u \right|_{\text{max}}} = \frac{\ddot{u}_o^t}{A}$$
 (5)

where \ddot{u}_o^t is the peak value of the total acceleration and A is the pseudo-acceleration (Chopra, 2007).

The response was computed for system natural vibration period between 0.1 sec and 5 sec, two values of damping ratio (5% and 10%), and a total of sixty ground accelerations (two horizontal components for each of the 30 selected ground motions). The ratio of the inertial and structural base shear, V_{bI}/V_{bR} , for each ground motions as well as the median value is presented in Figure 8.

The results presented in Figure 8 show that the inertial and structural base shears are

essentially identical for system with vibration period less that 1 sec for both damping ratios and all ground acceleration records: the ratio V_{bI}/V_{bR} is essentially equal to one for periods up to 1 sec. For longer system periods, however, the inertial base shear may exceed the structural base shear for a few ground accelerations as apparent from the ratio V_{bI}/V_{bR} being larger than one for few individual ground motions and system periods longer than 1 sec. The ratio V_{bI}/V_{bR} tends to be larger for larger damping which becomes apparent by comparing results in Figure 8a for 5% damping with those in Figure 8b for 10% damping. These observations are consistent with those reported previously by Chopra (2007: Section 6.12.2). The median of the V_{bI}/V_{bR} ratio varies very little from one for both damping ratios and all system periods.

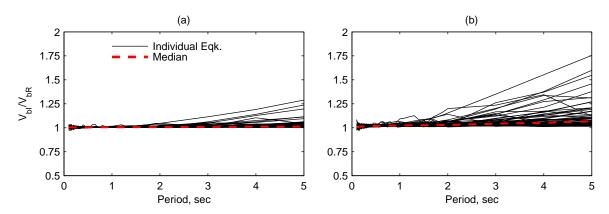


Figure 8. Ratio of inertial and structural base shear for linear-elastic SDF systems: (a) 5% system damping, and (b) 10% system damping.

The results for SDF system indicate that inertial base shear may be used as a good indicator of structural base shear for systems with vibration period shorter than about 1 sec. This observation is valid both for individual ground motions as well as for median computed for an ensemble of ground motions. For systems with periods longer than 1 sec, however, this observation is valid only for median computed for an ensemble of ground motions; inertial base shear may significantly exceed the structural base shear for systems with period longer than 1 sec for individual ground motions. Therefore, it is expected that the inertial base shear may exceed the structural base shear for long-period multi-story buildings for individual earthquake ground shaking.

Multistory Buildings

Compared in this section are the inertial and structural base shears in the two selected building for the selected ground motions. It is useful to note that the ground motions in Table 1 were not selected to match any design spectrum but to ensure that they will induce different levels of inelastic behavior in the selected buildings. It was found during RHA that the selected buildings experienced excessive deformation due to several of the ground motions and collapsed. For example, the North Hollywood Hotel collapsed for ground motions number 7 to 11, 13, 17, 18, 21, and 26, 29, and the Los Angeles Buildings collapsed due to ground motions number 5 to 11, 13, 17, 18, and 26 to 29. Results for these ground motions have been excluded from those presented in this section.

Examined first were the time-variations of inertial and structural base shears for selected ground motions. This examination showed that the inertial base shear matched the structural base shear quite well for some earthquakes but the difference was very large for others. Since the length limitation of this paper prohibit presentation of all results, selected results are presented for each of the two buildings in Figures 9 to 12 to demonstrate cases where the two base shears matched quite well and where they differed significantly.

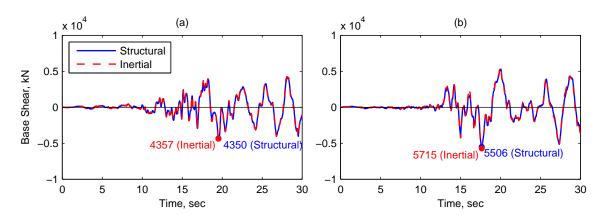


Figure 9. Comparison of inertial and structural base shears for North Hollywood Hotel for Earthquake No. 14: (a) Longitudinal direction, and (b) Transverse direction.

The results for the North Hollywood Hotel indicate that the inertial base shear tracks the structural base shear quite well for earthquake no. 14. Furthermore, the peak value of inertial base shear is essential equal to the structural base shear in the longitudinal direction (Figure 9a)

and exceeds the structural base shear by no more than 4% in the transverse direction (Figure 9b). While the inertial base shear tracks the structural base shear quite well for earthquake no. 9, the peak value may differ by about 10% in the longitudinal direction (Figure 10a) and by about 20% in the transverse direction (Figure 10b).

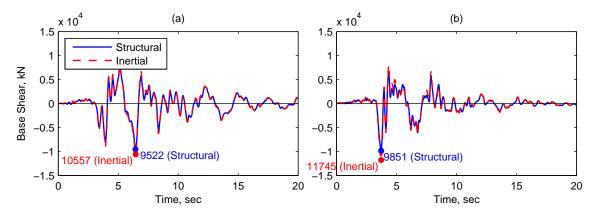


Figure 10. Comparison of inertial and structural base shears for North Hollywood Hotel for Earthquake No. 9: (a) Longitudinal direction, and (b) Transverse direction.

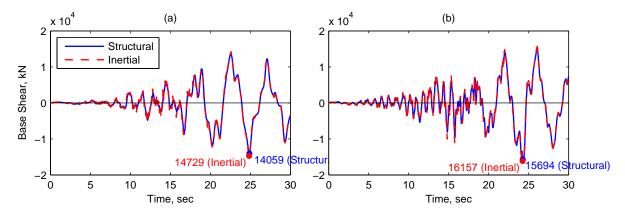


Figure 11. Comparison of inertial and structural base shears for Los Angeles Building for Earthquake No. 4: (a) Longitudinal direction, and (b) Transverse direction.

The results presented for the Los Angeles Building indicates a very good match between inertial and structural base shears for earthquake no. 4 (Figure 11). For earthquake no. 15, however, the inertial base shear differs significantly from the structural base shear not only in the peak value but frequency content as well (Figure 12). The peak value of inertial base shear exceeds the structural base shear by about 70% in the longitudinal direction (Figure 12a) and by about 35% in the transverse direction (Figure 12b). The results of Figure 12 also show that the

inertial base shear has significantly larger high-frequency content compared to the structural base shear. Therefore, it appears that the inertial base shear may significantly exceed the structural base shear for ground motions with very large high-frequency content.

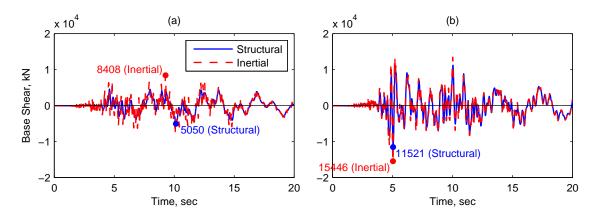


Figure 12. Comparison of inertial and structural base shears for Los Angeles Building for Earthquake No. 15: (a) Longitudinal direction, and (b) Transverse direction.

Examined next are the ratios, V_{bxI}/V_{bxR} and V_{byI}/V_{byR} , of the inertial and structural base shears for the two buildings. The results are presented in Figures 13 and 14 for earthquakes for which the building did not to collapse. The presented results include ratios, V_{bxI}/V_{bxR} and V_{byI}/V_{byR} , for individual earthquakes along with the median values.

The results presented in Figure 13 for the North Hollywood Hotel show that the ratio V_{bI}/V_{bR} for some earthquakes can be as high as 1.2. This indicates that inertial base shear may exceed the structural base shear by up to 20%. This observation is consistent with that noted previously for SDF systems with periods longer than 1 sec; the fundamental vibration period of this building is 2.57 sec in the longitudinal direction and 2.98 sec in the transverse direction. The median value of the ratio is, however, much smaller: the median ratio is from 1.07 (Figure 13a) to 1.11 (Figure 13b). Therefore, it may be expected that the inertial force will exceed the structural base shear in the median by about 5 % to 10%.

The results presented in Figure 14 for the Los Angeles building show that the median value of the ratio varies from 1.07 (Figure 14a) to 1.22 (Figure 14b) implying that the inertial base shear exceeds the structural base shear in the median by 5% to 20%. For individual earthquake,

the ratio can be as high as 1.7 in the longitudinal direction (Figure 14a) and 1.4 in the transverse direction (Figure 14b). This observation is consistent with that noted previously for SDF systems with periods longer than 1 sec; the fundamental vibration period of this building is 3.89 sec in the longitudinal direction and 3.42 sec in the transverse direction.

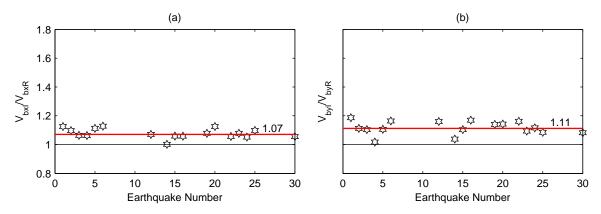


Figure 13. Ratio of peak inertial and structural base shears for North Hollywood Hotel: (a) Longitudinal direction, and (b) Transverse direction.

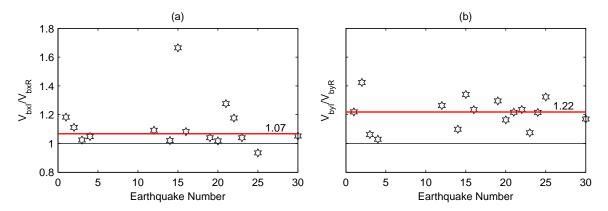


Figure 14. Ratio of peak inertial and structural base shears for Los Angeles Building: (a) Longitudinal direction, and (b) Transverse direction.

The discussion so far indicates that the median inertial base shear exceeds the structural base shear by 10 to 20%. For individual earthquakes, however, the inertial base shear may exceed the structural base shear by as much as 70%. The observation for individual ground motions is consistent with the prediction from SDF results where it was found that the inertial base shear may exceed the structural base shear for long-period systems. Furthermore, the large discrepancy between inertial and structural base shears occurs for ground motions with very large high-frequency content. Therefore, inertial base shear should be used with caution as an estimate of

the structural base shear in buildings with motions recorded during earthquake ground shaking.

It is useful to recall that the discrepancy between the inertial base shear estimated from recorded motions during the 1994 Northridge earthquake and structural base shear estimated form the pushover analysis for the two selected buildings was found to be much larger in Figures 2 and 3 compared to the observations from Figures 13 and 14. As mentioned previously, the larger discrepancy in the former case may be due to combination of inaccuracies arising in estimation of the inertial base shear from interpolation of motions recorded at limited number of floors to obtain motions and remaining floors, and modeling assumptions in computer model to estimate the structural base shear.

CONCLUSIONS

This investigation examined if the inertial base shear, defined as summation of floor inertial forces above the building's base with the floor inertial forces computed by multiplying the floor masses with the total floor accelerations, can provide an accurate estimate of the structural base shear which is equal to sum of shears in all columns at the building's base. It was found for SDF systems responding in the linear elastic range that the inertial base shear may be used as a good indicator of structural base shear for systems with vibration period shorter than about 1 sec. For systems with periods longer than 1 sec, however, the inertial base shear may significantly exceed the structural base shear for individual earthquake ground motions.

It was found for multi-story buildings that the median inertial base shear exceeds the structural base shear by 10 to 20%. For individual earthquake ground motions, however, the inertial base shear may exceed the structural base shear by as much as 70%. It was also found that the large discrepancy between inertial and structural base shears occurs for ground motions with very large high-frequency content. Therefore, inertial base shear should be used with caution as an estimate of the structural base shear for individual ground motion, in particular for building with long fundamental vibration periods.

REFERENCES

- ASCE, 2000. Prestandard and Commentary for the Seismic Rehabilitation of Buildings. *Report No. FEMA-356*, Building Seismic Safety Council, Federal Emergency Management Agency, Washington, D.C.
- Chopra, A., 2007. Dynamics of Structures: Theory and Applications to Earthquake Engineering, 3rd Edition, New Jersey: Prentice Hall.
- CSI, 2006. Perform3D: Nonlinear Analysis and Performance Assessment for 3d Structures: Version 4. Computers and Structures, Inc., Berkeley, CA. <www.csiberkeley.com)>
- De la Llera, J. C. and Chopra, A. K., 1998. "Evaluation of Seismic Code Provisions Using Strong-Motion Building Records from the 1994 Northridge Earthquake," *Report No. UCB/EERC-97/16*, Earthquake Engineering Research Center, University of California, Berkeley, CA.
- Goel, R.K., 2005. "Evaluation of Modal and FEMA Pushover Procedures Using Strong-Motion Records of Buildings," *Earthquake Spectra*, **21**(3): 653-684, 2005.
- Goel, R.K. and Chadwell, C., 2007. "Evaluation of Current Nonlinear Static Procedures for Concrete Buildings Using Recorded Strong-Motion Data," *CSMIP Data Interpretation Report*, Strong Motion Instrumentation Program, CDMG, Sacramento, CA.
- Goel, R.K., 2008. "Mode-Based Procedure to Interpolate Strong Motion Records of Instrumented Building," *Technical Note, ISET Journal of Earthquake Technology*, **45**(3-4): 97-113.
- Jennings, P. C., 1997. "Use of Strong Motion Data in Earthquake Resistant Design," Proceedings of SMIP97 Seminar on Utilization of Strong-Motion Data, Strong Motion Instrumentation Program, CDMG, Sacramento, CA.
- Limongelli, M. P., 2003. "Optimal Location of Sensors for Reconstruction of Seismic Response through Spline Function Interpolation," *Earthquake Engineering and Structural Dynamics*, **32**(7):1055-1074.
- Limongelli, M.P., 2005. "Performance Evaluation of Instrumented Buildings," *ISET Journal of Earthquake Technology*, **42**(2-3):47-61.
- Naeim, F., 1997. Performance of Extensively Instrumented Buildings During the January 17, 1994. Northridge Earthquake: An Interactive Information System, *Report No. 97-7530.68*, John A.

- Martin & Associates, Los Angeles, CA, 1997.
- Naeim, F., 1998. "Performance of 20 Extensively-Instrumented Buildings during the 1994 Northridge Earthquake," *The Structural Design of Tall Buildings*, **7**(3): 179-194.
- Naeim, F., Lee, H., Bhatia, H., Hagie, S., and Skliros, K., 2004. "CSMIP Instrumented Building Response Analysis and 3-D Visualization System (CSMIP-3DV)," *Proceedings, SMIP04 Seminar on Utilization of Strong-Motion Data*, Strong Motion Instrumentation Program, CDMG, Sacramento, CA.
- Shakal, A., Huang, M., and Graizer, V., 2003. Strong-Motion Data Processing, International Handbook of Earthquake Engineering Seismology, Academic Press, Edited by Lee, Kanamori, Jennings, and Kisslinger, Part B, 81B:967-981.
- TRC, 2008, Cross Sectional Analysis of Structural Components, v3.0.8, TRC/Imbsen Software Systems, Rancho Cordova, CA. http://www.imbsen.com/